Observation of Near-Forward Stimulated Brillouin Scattering from a Laser-Produced Plasma

S. H. Batha,[1],[a] K. S. Bradley,[2],[3] H. A. Baldis,[2] R. P. Drake,[1],[3] Kent Estabrook,[2]
T. W. Johnston,[4] and D. S. Montgomery[2]

[1]*Plasma Physics Research Institute, University of California, Davis, California 95616 and Lawrence Livermore National Laboratory, Livermore, California 94550*
[2]*Lawrence Livermore National Laboratory, Livermore, California 94550*
[3]*Department of Applied Science, University of California, Davis, California 95616*
[4]*Institut National de la Recherche Scientifique–Énergie, Varennes, Québec, Canada J3X1S2*
(Received 28 May 1992)

The first experimental measurements of near-forward scattering from a plasma at wavelengths near the pump wavelength are presented. Simultaneous, time-resolved spectra from several oblique forward angles show the characteristic wavelength shift associated with scattering from an ion wave. Energy measurements show that forward scattering is stronger than backscattering. The angular distribution of forward scattered energy is in qualitative agreement with the simple convective-instability theory of stimulated Brillouin scattering.

PACS numbers: 52.35.Nx, 52.35.Mw, 52.40.Nk

Stimulated Brillouin scattering (SBS) is a parametric instability whereby a pump wave couples to an acoustic phonon and an electromagnetic (em) wave. SBS is an important phenomenon in both nonlinear optics [1] and plasma physics [2] because a large fraction of the incident pump energy may be scattered by the instability. Thus SBS is an issue in any application in which a sufficiently large fluence of electromagnetic energy penetrates an optical medium. In plasma physics, SBS is a significant consideration for laser-driven inertial-confinement fusion (ICF) because of its potential to decrease the amount of energy absorbed and to decrease implosion symmetry. Backscattered SBS, where the em wave is directed antiparallel to the pump, has been extensively studied in plasmas because it has the largest growth rate in a homogeneous plasma. Near-forward SBS (NFSBS), where the wave vectors of the em and the ion-acoustic (IA) waves have components parallel to the pump wave, although predicted [3], has not previously been observed.

Near-forward SBS can, in principle, move the laser-heating region, thereby ruining symmetry in both direct- and indirect-drive ICF. Sufficient ion heating can stabilize Brillouin by Landau damping. Manley and Rowe describe the partition of energy into em and IA (heating) energy by the ratio ω_S/ω_{IA}. However, the NFSBS ion heating rate is an order of magnitude smaller than backscattering because the IA wave number is small for forward scattering. Brillouin backscattering can heat ions to reduce NFSBS in the same place. In indirect drive, plasma from the hohlraum walls can collide along the center line, providing substantial, cheap ion heating to help suppress SBS in all directions.

The results of experiments designed to detect the presence of NFSBS and also to test convective theory are presented. Reflections from the n_c surface [4] and ion-acoustic turbulence at the $n_c/4$ and n_c surfaces may alter the behavior of SBS [5]. (The critical density n_c is where the laser and plasma frequencies are equal.) Stimulated Raman scattering (SRS) may interact with SBS [6] and further complicate the analysis. In order to minimize these complications, a preformed plasma approach was chosen [5]. The plasma was of low enough density during the period of SBS emission that there was no n_c or $n_c/4$ surface and that SRS backscattering was Landau damped.

The experiment was similar to one used to investigate forward SRS [7–9] and the specific problems of designing an experiment for SBS and of measuring the SBS are discussed in Ref. [10]. Titanium foils which were 0.5 ± 0.025 μm thick, 1.65 ± 0.1 mm in diameter, and mounted on a 1000-Å Formvar support, were irradiated on each side by four "preforming" beams of the NOVA laser system [11]. The eight preforming beams had a nominal energy at 351 nm of 22 kJ in a 2-nsec-square pulse, with nominal rise and fall times of 100 psec. Each beam was focused with $f/4.3$ optics and was incident on the foil at a 50° angle from normal incidence. The resulting overlap region was roughly circular with a FWHM of 850 μm. A ninth beam was used as an interaction beam to drive the instability. It operated at 527 nm and was delayed 1.8 nsec after the start of the preforming beams, overlapping the preforming beams by 200 psec. The energy of the interaction beam was 0.16 ± 0.05 kJ. A mid-Z plasma was chosen so that the quantity ZT_e/T_i (where T_e and T_i are the electron and ion temperatures, respectively) would be large, guaranteeing initially low ion-wave damping.

The primary diagnostic was the multiple-angle, time-resolving spectrometer (MATRS) [12]. MATRS consists of six collectors placed inside the NOVA target chamber and one collector, using a splitter, in the interaction-beam path to measure direct backscattering. Seven simultaneous, calibrated, time-resolved spectra were recorded with a streak camera on a single irradia-

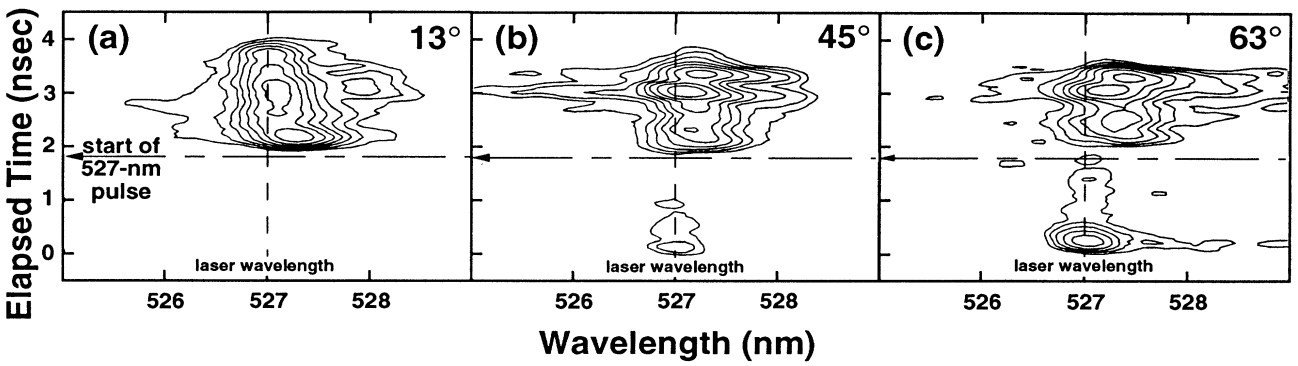

FIG. 1. Time-resolved spectra near the fundamental laser frequency at three angles from the forward direction of the pump laser: (a) 13°, (b) 45°, and (c) 63°. The isointensity contours are separated by a factor of 2 in spectral intensity with the highest contour at 90% of the maximum intensity in each spectrum.

tion, with typical resolutions of 100 psec and 4 Å, although shifts in peak location as small as 1 Å may be observed. The spectral intensity of each channel was absolutely calibrated by a time-integrated photodiode adjacent to each light collector inside the chamber. Other diodes, for a total of 25, were used to determine the angular distribution of scattered light corresponding to SBS from the interaction beam. Forward SRS was looked for, but not observed, and backscattered SRS was seen only rarely in a short burst at the start of the interaction-beam pulse.

The forward-scattered SBS spectra are presented in Fig. 1. In this irradiation, the nominal plasma properties, at 2.2 nsec after the start of the preforming beams, were estimated using a 2D hydrocode [13] to be the following: peak density of $0.04n_c$, density profile FWHM of 1.2 mm, velocity gradient of 7.5×10^8 sec^{-1}, electron temperature of 2.6 keV, $ZT_e/T_i > 22$, and sound speed of 3.5×10^7 cm/sec. Experimental measurements have shown that the density could be a factor of 2 higher and T_e a factor of 2 lower [8,14]. The instantaneous incident laser intensity was 6×10^{13} W/cm^2 at 2.2 nsec, defined to be the average in a (175 ± 30)-μm-diam spot which contains 80% of the incident laser energy. Further details of the plasma quantities, including a discussion of the uncertainties, will be published [14]. The narrow emission beginning at time=0 in Figs. 1(b) and 1(c) is 527-nm light created as a by-product of the frequency tripling process of the preforming beams that is scattered from the target stalk [12]. Each signal begins promptly (to within the accuracy of the measurement) when the interaction beam begins at 1.8 nsec. Emission from the most-forward channel lasts the duration of the interaction beam pulse. The emission is shorter from the 45° channel and shortest from the 63° channel, the most nearly sidescattered. The full width can be as large as 13 Å (at 10% of the maximum intensity of each spectrum), as in the case of the most-oblique detector, Fig. 1(c). The peak emission is also seen to be shifted to longer wavelengths, with the largest shifts, as expected from SBS from a subsonic plasma, at the beginning of the pulse. The intensity of the signal varies smoothly in time, but within the resolution varies much less in time than in angle. Similar spectra were obtained with both higher laser intensities and higher peak plasma densities.

The angular distribution of scattered-light energy is presented in Fig. 2(a). Each data point is the average of three experiments with similar irradiations, while the extent of the bars corresponds to the range of values in the three irradiations. The error in each measurement is estimated to be $\pm20\%$. Reproducibility between irradiations is within a factor of 2, which is typical for this type of measurement [15]. The most striking aspect of these data is the high scattering efficiency in the forward direc-

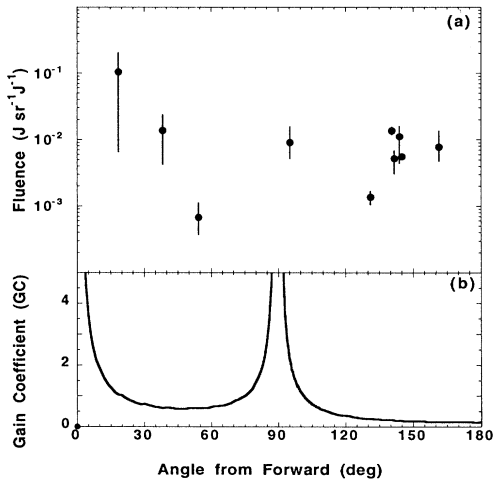

FIG. 2. (a) The angular distribution of scattered light as measured by time-integrated photodiodes. (b) The convective gain coefficient as a function of angle computed using Eq. (1). Plasma parameters are those given in the paper with $T_i=2.5$ keV, $Z=20.5$, and zero flow velocity.

tion. With the exception of the measurements at 90°, the angular distribution peaks in the forward and backward directions with a drop of 2 orders of magnitude in between. At 90°, the scattering efficiency is again apparently high. However, there are too few detectors in this sector to make any quantitative estimates of sidescattering, or of any trends. Direct backscattering measurements are not reported because of energy calibration problems [10]. Data from other experiments using a higher laser intensity, a higher density plasma, or both, followed the same trends as depicted in Fig. 2(a).

The scattered-light intensity of convectively amplified SBS grows exponentially from thermal noise sources as $I_{\text{scat}} = I_{\text{noise}} \exp(C_{\text{gain}})$, where C_{gain} is the gain coefficient. For a linear phase-mismatch plasma profile with damping of the daughter waves, Williams [16] has calculated the intensity exponential gain coefficient to be

$$C_{\text{gain}} = \frac{2\pi\gamma_0^2}{|\kappa' V_{g,\text{IA}} V_{g,\text{em}}|} \frac{2}{\pi} [\arccos(G) - G(1-G^2)^{1/2}] , \quad (1)$$

where κ' is the derivative of the wave-number mismatch, and $V_{g,\text{IA}}$ and $V_{g,\text{em}}$ are the components of the group velocities of the IA and em waves along the direction of inhomogeneity. The argument $G \equiv (\nu_{\text{IA}}\nu_{\text{em}})^{1/2}/\gamma_0$, where ν_{IA} and ν_{em} are the damping rates on the IA and em waves, respectively. The reduction due to damping in this experiment is only a few percent. For this calculation, and for clarity, it has been assumed that the directions of the flow gradient, density gradient, and pump are collinear. The homogeneous growth rate γ_0 is proportional to k_{IA}, the magnitude of the IA wave number which decreases to zero for direct forward scattering. However, the denominator of Eq. (1) also vanishes for forward scattering. In order to understand the results of Fig. 2(a), the values of C_{gain} have been calculated from Eq. (1) and are displayed in Fig. 2(b). Following the curve from backscatter towards sidescatter, the gain monotonically increases. There is a singularity at sidescattering where $V_{g,\text{em}}$ is orthogonal to the phase inhomogeneity direction and WKB theory breaks down. As the scattering angle is further decreased, the gain first decreases away from the singularity to a minimum at about 50° where the gain coefficient is about 4 times the backscattering value. Near-direct forward scattering is large because of the singularity where $V_{g,\text{IA}}$ is orthogonal to the phase inhomogeneity direction. The data of Fig. 2(a) are in qualitative agreement with a convective amplifier model, Fig. 2(b), although the data do not yet allow a detailed comparison with this model. The data show a stronger backscattering component which may be due to an absolute instability being excited in this direction [10].

The wavelength shift of the SBS light from the laser wavelength versus scattering angle is presented in Fig. 3. For the forward channels, the wavelength of peak emission is plotted, while for the backward channels, the wavelength of the redshifted satellite is plotted. The backscattered spectra, shown in Ref. [10], have other structure as well. In cases without a distinct peak, the range of shifts has been plotted with a shaded bar. At the two times shown, the wavelength shift of each of the forward channels is 3 Å or less. The backscatter channels have larger shifts, of the order of 8 to 20 Å. The forward-angle shifts become smaller later in the interaction beam pulse. Also plotted in Fig. 3 are predictions for the wavelength shift derived by solving the dispersion relations and energy and momentum conservation conditions for the three waves, including flow, for scattering from the zero-flow region and also from a region 500 μm behind the center of the plasma, corresponding to the end of the beam waist. Calculations for 500 μm in front of the center show a blueshift of less than 5 Å. The observed shifts are consistent with SBS if it is assumed that scattering at each angle originates at a different physical location in the plasma. This would not be a surprising nonlinear development because scattering into different angles changes the magnitudes of the group velocities of the IA and em waves along the phase gradient, the important quantities in the Rosenbluth gain formula. From Fig. 3, it may be inferred that scattering at angles $> 90°$ originates from regions where the flow is parallel to the laser direction, while scattering in the forward direction originates in regions where the flow is antiparallel to the laser.

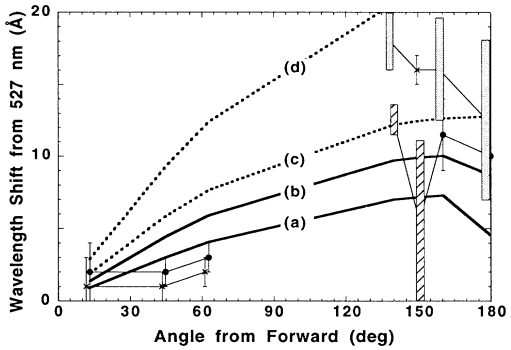

FIG. 3. Shift of the scattered spectrum at 2.2 (●) and 3.0 nsec (×). The data at 3.0 nsec have been shifted by −1.5° for legibility. Forward (backward) spectra were averaged over 120 (280) psec. The shaded bars indicate the range of enhanced emission when no distinct peak was apparent. The solid (dotted) curves are the theoretical predictions for zero (nonzero) flow, at the center of the plasma (500 μm closer to the laser). Curves *a* and *c* are for the parameters appropriate to the plasma conditions at 2.2 nsec, while curves *b* and *d* are appropriate to 3.0 nsec. This calculation assumed that the laser was incident at 50° to the collinear velocity and density gradients in order to more correctly model the experiment. Note that there is also an uncertainty in the angle between k_{IA} and the flow direction in the actual interaction region.

We have analytically and computationally tested two other explanations of the data, recalling that a satisfactory theory must explain both the scattered-light spectra and the angular distribution of scattered energy. The first supposes that a time-varying optical path in the plasma causes a frequency shift [17,18] and that refraction or reflection scatters the energy into a wide range of angles. Postprocessing of a 2D simulation shows that the calculated shift is of the same order as the data; however, simulation noise makes comparison difficult. A model calculation predicts that spherical plasma expansion would produce a larger wavelength shift (0.7 Å) than a longitudinal expansion (0.3 Å). One expects the smaller shift since the simulation shows that the flow is still dominantly longitudinal and the density is low. Scattering at an angle (i.e., 63°) would not increase the shift unless the flow were primarily transverse. Thus, the predicted shifts due to this effect overlap with the error bars at 13° and 45°, but are in conflict with the result at 63°. Simulations show that the density is too low to refract the laser beam by more than a few degrees. Fresnel reflection from density interfaces in the plasma was also examined. Approximately 3000 randomly oriented large interfaces, each intercepting 10% of the laser beam at angles up to 30° from the laser direction, would be needed to explain the observed signal level and angular distribution. This seems unlikely given that the plasma size is only of the order of 3000 μm.

The second phenomenon examined was filamentation. The laser intensity is near threshold for filaments to form in the plasma. As the laser exits a filament, the light may scatter in many directions [19]. While a static filament produces no frequency shift, a dynamic filament certainly will, in principle, but the question remains as to just how much spectral shift one should expect. In order to match the smoothly varying wavelength shift of the spectra shown in Fig. 1, the features involved (such as a filament boundary) must move at something like the sound velocity for times comparable to the signal duration all in such a way as to produce mostly redshifts rather than blueshifts. Such structures are implausible. A more detailed analysis is beyond the scope of this Letter, since it would require tracing the dynamic phase behavior of the exit light in a well-developed realistic filament model, such as that of Schmitt [20].

This Letter has reported the first measurement of near-forward stimulated Brillouin scattering from a laser-produced plasma. This claim is based on time-resolved spectra, simultaneously collected at three angles, which show a wavelength shift consistent with SBS. The angular distribution of scattered light was measured and is in qualitative agreement with convective amplification in a linear phase-mismatch profile. Time-integrated photodiodes show that NFSBS is stronger than backscattered SBS.

The authors would like to acknowledge useful discussions with K. L. Baker, R. L. Berger, E. Hsieh, W. L. Kruer, J. D. Moody, S. C. Wilks, and E. A. Williams and the efforts of the NOVA operations group. This work was performed under the auspices of the U.S. Department of Energy by the Lawrence Livermore National Laboratory under Contract No. W-7405-ENG-48.

---

[a]Present address: Fusion Physics and Technology, Torrance, CA 90503.

[1] R. W. Boyd, *Nonlinear Optics* (Academic, Boston, 1992).
[2] S. E. Bodner, J. Fusion Energy **1**, 221 (1981).
[3] G. R. Mitchel, T. W. Johnston, and B. Grek, Phys. Fluids **25**, 186 (1982).
[4] C. J. Randall, J. J. Thomson, and K. G. Estabrook, Phys. Rev. Lett. **43**, 924 (1979).
[5] P. E. Young, H. A. Baldis, and K. G. Estabrook, Phys. Fluids B **3**, 1245 (1991).
[6] D. M. Villeneuve, H. A. Baldis, and J. E. Bernard, Phys. Rev. Lett. **59**, 1585 (1987).
[7] S. H. Batha *et al.*, Phys. Rev. Lett. **66**, 2324 (1991).
[8] S. H. Batha *et al.*, Phys. Fluids B **3**, 2898 (1991).
[9] S. H. Batha *et al.* (to be published).
[10] K. S. Bradley *et al.* (to be published).
[11] E. M. Campbell *et al.*, Rev. Sci. Instrum. **57**, 2101 (1986).
[12] K. S. Bradley *et al.*, Rev. Sci. Instrum. **63**, 5205 (1992).
[13] G. B. Zimmerman and W. L. Kruer, Comments Plasma Phys. Controlled Fusion **2**, 51 (1975).
[14] S. H. Batha *et al.* (to be published).
[15] R. P. Drake *et al.*, Phys. Fluids B **1**, 1295 (1989).
[16] E. A. Williams, Phys. Fluids B **3**, 1504 (1991).
[17] A. Bonnier, Ph.D. thesis, Universite du Quebec, 1973 (unpublished).
[18] T. Dewandre, J. R. Albritton, and E. A. Williams, Phys. Fluids **24**, 528 (1981).
[19] K. Estabrook, W. L. Kruer, and D. S. Bailey, Phys. Fluids **28**, 19 (1985).
[20] A. J. Schmitt, Phys. Fluids B **3**, 186 (1991).